Since January 2020 Elsevier has created a COVID-19 resource centre with free information in English and Mandarin on the novel coronavirus COVID-19. The COVID-19 resource centre is hosted on Elsevier Connect, the company's public news and information website.

Applied Catalysis B: Environmental 317 (2022) 121709

Contents lists available at ScienceDirect

Applied Catalysis B: Environmental

journal homepage: www.elsevier.com/locate/apcatb

The role of trace N-Oxyl compounds as redox mediator in enhancing antiviral ribavirin elimination in UV/Chlorine process

Qiyuan Sun [a,d,1], Jing Yang [a,1], Yongjie Fan [a], Kaicong Cai [b,c], Zhilei Lu [a], Zhenle He [a], Zeping Xu [a], Xingteng Lai [a], Yuyi Zheng [a], Changqing Liu [a], Feifeng Wang [a,d,*], Zhe Sun [e,**]

[a] College of Environmental Science and Engineering, Fujian Normal University, Fuzhou, Fujian 350007, China
[b] College of Chemistry and Materials Science, Fujian Provincial Key Laboratory of Advanced Materials Oriented Chemical Engineering, Fujian Normal University, Fuzhou 350007, China
[c] Fujian Provincial Key Laboratory of Theoretical and Computational Chemistry, Xiamen 361005, China
[d] Fujian Key Laboratory of Pollution Control & Resource Reuse, Fuzhou, Fujian 350007, China
[e] Key Laboratory of Drinking Water Science and Technology, Research Center for Eco-Environmental Sciences, Chinese Academy of Sciences, 18 Shuang-qing Road, Beijing 100085, China

ARTICLE INFO

Keywords:
Ribavirin
N-oxyl compounds
TEMPO
NHPI
UV/Chlorine

ABSTRACT

Ribavirin (RBV) is an antiviral drug used for treating COVID-19 infection. Its release into natural waters would threaten the health of aquatic ecosystem. This study reports an effective approach to degrade RBV by the trace N-oxyl compounds (2,2,6,6-tetramethylpiperidine-N-oxyl (TEMPO) and N-Hydroxyphthalimide (NHPI)) enhanced UV activated free chlorine (UV/Chlorine) process. The results indicated that TEMPO and NHPI at low concentrations (0.1 μM and 1 μM, respectively) could strongly enhance RBV degradation in both deionized water with different pHs and practical surface water. The enhancement was verified to be attributed to the transformation of TEMPO and NHPI into their reactive forms (i.e., $TEMPO^+$ and PINO), which generations deeply relied on radicals. The two N-oxyl compounds inhibit ClO• yield by hindering the reaction of free chlorine vs. HO• and Cl•. The analyses on acute toxicities of RBV degradation products indicate that UV/Chlorine/N-oxyl compounds process can detoxify RBV more efficiently than UV/Chlorine process.

1. Introduction

Ribavirin (RBV, molecular structure illustrated in Fig.S1) has been widely used in clinical treatments for antiretroviral therapy. In responding to the rapid spread of the Corona Virus Disease 2019 (COVID-19) pandemic, RBV was recommended by World Health Organization (WHO) to treat the infections caused by COVID-19 [1]. Along with the heavy usage, RBV will inevitably be discharged into the natural surface water. The concentrations of RBV detected in rivers near hospitals of Jinyintan, Huoshenshan and Leishenshan in Wuhan, China, were higher than those reported in historical studies, which might threaten aquatic organisms [2]. According to the Predicted No-Effect Concentrations (PNEC) analyses for aquatic organisms (e.g., green algae, daphnia, and fish), RBV has a higher chronic toxicity than other antiviral drugs such as ritonavir, chloroquine, and rapamycin. Algae appeared to be the most sensitive species to RBV based on Risk quotient (RQ) analysis [3,4]. As such, it is necessary to remove the RBV in natural surface water to minimize its adverse impact on aquatic ecosystem security.

Several processes have been proposed to remove RBV in water. Most of them belong to advanced oxidation processes (AOPs), such as homogeneous photocatalysis using ozone/PMS, Fenton-like system, and heterogeneous photocatalysis using nanoscale Bi_4VO_8Cl [5–8]. Among these processes, ultraviolet light activated free chlorine (hereafter referred to UV/Chlorine) process appears to be one of the most attractive technologies. UV/Chlorine process has been widely used for drinking water disinfection and sewage treatment, which can remove pollutants by direct UV photolysis, oxidations by free chlorine and hydroxyl radical (HO•), as well as a series of reactive chlorine species (RCS) [9]. However, the degradation performances of UV/Chlorine process toward

* Corresponding author at: College of Environmental Science and Engineering, Fujian Normal University, Fuzhou, Fujian 350007, China.
** Corresponding author.
E-mail addresses: wffeng@fjnu.edu.cn (F. Wang), zhesun@rcees.ac.cn (Z. Sun).
[1] These authors contributed equally to this work.

https://doi.org/10.1016/j.apcatb.2022.121709
Received 22 April 2022; Received in revised form 19 June 2022; Accepted 3 July 2022
Available online 5 July 2022

different pollutants are largely determined by the second order rate constants of the reactions between radicals and pollutants. RBV, with a relatively low second order rate constant of HO• vs. RBV ($1.2–1.9 \times 10^9$ $M^{-1}\cdot s^{-1}$), is difficult to be decomposed because of its dual-heterocyclic conjugate structure [5]. Thus, it is necessary to modify UV/Chlorine process to enhance the RBV degradation.

Redox mediator can enhance pollutants degradation by AOPs in at least two ways. In one way, it can act as an "electron shuttle" to promote the electron transfer, which increases the yield of AOPs derived radicals. In the other way, it can be oxidized by oxidants, and transformed into reactive intermediate, which can degrade pollutants by extracting their hydrogen atoms or oxidizing their hydroxyl groups [10,11]. The traditional redox mediators can be divided into three categories, which are carbon redox mediators, transition metal redox mediators, and metal porous carbon composite redox mediators [12,13]. In recent years, trace organic redox mediators have been proposed. Nonetheless, there are only few researches focused on this field, which has limited their applications in the improvement of pollutants degradation by AOPs [14–17].

N-Oxyl compounds, such as 2,2,6,6-tetramethylpiperidine-N-oxyl (TEMPO) and N-Hydroxyphthalimide (NHPI), have been widely used as catalysts or redox mediators in polymerization reactions [18,19]. TEMPO could be oxidized into N-oxoammonium ion ($TEMPO^+$) by an electrochemical process, which serves as an active catalytic species that can react readily with secondary hydroxyl group to produce carbonyls [19]. NHPI, likewise, could also be oxidized into phthalimide N-oxyl (PINO), which is conductive to extract hydrogen atoms from relatively weak C-H bonds in the functional groups such as allyl and benzyl groups [19–22]. Recent literatures mentioned that $TEMPO^+$ derived from TEMPO by Mn(VII) oxidation could degrade organic pollutants, and isopropylbenzene could also be oxidized by the system of NHPI, Fe $(acac)_3$ and 1,10-phenanthroline [19,23]. However, currently the N-Oxyl redox mediators are mainly used in non-illuminated AOPs, such as Fenton-like processes or electrochemical processes. Little attention is paid to the application of N-Oxyl redox mediator in illuminated AOPs (e.g., UV/Chlorine process) to enhance pollutants removal efficiency. Also, the associated degradation mechanisms, such as the effects of N-Oxyl redox mediator on the generation of radicals and degradation pathway, are still unclear.

N-Oxyl-compounds (e.g., TEMPO and NHPI) have been widely used not only in catalysis field, but also in biomedical field. Several literatures have reported that TEMPO is a relatively safe antioxidant when it is applied at low concentrations (< 0.1 mM), and has no significant effects on cell survival, glutathione (GSH) level, or the expression of apoptosis signal pathway molecules [24,25]. Similarly, NHPI can selectively inhibit the proliferation of breast cancer cells in the concentration range of 0–40 μM. When NHPI was applied to mice with tumors at a dose of 40 $mg\bullet kg^{-1}$ for 53 days, it not only showed no adverse effects on the body weights of mice, but also inhibited tumor growth by 53%, indicating that it is safe to use trace amount of NHPI in organisms [26,27]. Meanwhile, according to ECOSAR analysis, the LC50 (median lethal concentration) of TEMPO and NHPI for fish are 680 μM and 180 μM, respectively. Therefore, it can be deduced that there will not be harmful effect of using trace amount TEMPO and NHPI in UV/Chlorine process to remove contaminants.

The key hypothesis of this study is that the two N-Oxyl redox mediators (i.e., TEMPO and NHPI) can be served as electron shuttles or reactive intermediates to enhance the degradation of RBV by UV/Chlorine process. To test this hypothesis, the second-order rate constants of a series of radicals vs. RBV were determined. Then, the kinetics of RBV degradation by UV/Chlorine process in the absence and presence of N-Oxyl redox mediators were investigated, and the effects of pH, DOM, anions, and practical surface water on RBV degradation by this process were elucidated. Afterward, the radical-based degradation mechanisms of RBV by UV/Chlorine process were explored. Finally, the toxicities of RBV and its degradation products were assessed by ECOSAR analysis.

2. Materials and methods

2.1. Chemicals

Sources of chemicals are detailed in supporting information (SI Text S1).

2.2. Experimental procedures

The UV lamp consisted of a series of LED beads that mainly emit at the wavelength of 254 nm. The UV fluence (I_0) delivered to the reaction solution was measured by KI/KIO_3 actinometry [28]. The output spectrum of UV lamp was measured by a spectrometer (in SI Fig.S2) (Ocean optics, USB-4000). Prior to irradiation, UV lamp was preheated for at least 30 min to ensure the stability of UV radiation.

The photodegradation of RBV by UV/Chlorine process was conducted as the following steps. Prior to UV irradiation, 1 mL RBV (1 $g\cdot L^{-1}$) was spiked into a cylindrical jacketed reaction dish that pre-filled with 50 mL of 10 mM phosphate buffer (pH = 7.0). Then, the solution was diluted to 99 mL with deionized (DI) water. A quartz plate was used to cover the dish to prevent evaporation and allow the full penetration of UV light. An off-line condensing device was used to control the temperature of condensate flowing through the interlayer of the reaction dish to provide a stable temperature in the reaction system at 25 °C. Then, a magnetic stirrer was placed below the reaction dish to make sure the solution was well mixed. Afterward, 1 mL NaOCl stock solution (free chlorine = 4.2 mM as Cl_2) was spiked into the solution. As such, the solution in the reaction dish contained 10 $mg\cdot L^{-1}$ RBV and 42 μM free chlorine. Then, the photodegradation was started immediately after the stirred reaction dish was placed under the UV beam, with the irradiation time of 0 s. During the irradiation, samples were collected at each predetermined time interval. For each sample collection, 1 mL solution was collected from the reaction dish and filtered through a 0.22 μm membrane filter to remove impurities. The filtrate was immediately transferred to an amber vial that was pre-filled with 0.1 mg sodium sulfite to quench all the radicals and oxidants. At last, all the samples were stored at − 5 °C before analysis. It should be mentioned that the free chlorine concentration of NaOCl stock solution was recalibrated prior to each experiment.

The experiments of RBV photodegradation by UV/Chlorine/TEMPO and UV/Chlorine/NHPI processes were conducted to investigate how redox mediators could affect the kinetics and mechanisms of photodegradation. In these experiments, 9 groups of phosphate buffered RBV solutions (Phosphate buffer: 10 mM, RBV: 1 $g\cdot L^{-1}$) were spiked with 0, 0.5, 1, 2 mL TEMPO (10 μM) and 0, 0.1, 1, 3, 5 mL NHPI (100 μM), respectively. Then each solution was diluted to 99 mL with DI water and spiked with 1 mL NaOCl (free chlorine = 4.2 mM as Cl_2) before UV irradiation. Thus, the final concentrations of TEMPO in the first four groups were 0, 0.05, 0.1, and 0.2 μM, respectively, whereas the concentrations of NHPI in the last five groups were 0, 0.1, 1, 3, and 5 μM, respectively. Other procedures were same as the experiments of RBV photodegradation by UV/Chlorine process.

Steady state concentrations of various radicals, including hydroxyl radical (HO•), chlorine radical (Cl•), dichloride radical ($Cl_2^{\bullet-}$), and chlorine monoxide radical (ClO•), were estimated by radical scavenging experiments, which were conducted by adding probe compounds into the reaction solutions and use TBA (10 mM) to remove HO•, Cl•, ClO•, as well as other relative reactive intermediates. Other procedures were same as the experiments of RBV photodegradation by UV/Chlorine process.

To evaluate the effect of pH on the degradation of RBV by UV/Chlorine and UV/Chlorine/Redox mediator processes, experiments were conducted following the same experimental procedures for RBV photodegradation by UV/Chlorine process except that phosphoric acid, phosphate, and borate buffer solutions were added before UV irradiation to adjust the pH of the reaction solutions to 4.0, 5.0, 6.0, 7.0, 8.0, 9.0 and

10.0, respectively.

To evaluate the effect of dissolved organic matter (DOM), Cl^-, and HCO_3^-on the degradation of RBV by the UV/Chlorine and UV/Chlorine/Redox mediator processes, experiments were conducted following the same experimental procedures for RBV photodegradation by UV/Chlorine process except that Suwannee River natural organic matter (SRNOM), $NaHCO_3$, and NaCl were added into the reaction solution before UV irradiation, to adjust the concentrations of: SRNOM to 2 $mgC{\cdot}L^{-1}$, 5 $mgC{\cdot}L^{-1}$, and 10 $mgC{\cdot}L^{-1}$; HCO_3^- to 0.5 mM, 1 mM, and 3 mM; Cl^- at 5 mM, 10 mM, and 20 mM, respectively.

To reveal how different water matrix components in practical surface waters affect the degradation of RBV by the UV/Chlorine and UV/Chlorine/Redox mediator processes, experiments were conducted following the same experimental procedures for RBV photodegradation by UV/Chlorine process except that two types of practical surface waters collected locally were used as alternative to DI water. The geographical sampling sites and the water qualities of the two surface waters are shown in Fig. S42 and Table S1, respectively.

The oxidation products of TEMPO and NHPI were determined by electron paramagnetic resonance (EPR) at room temperature, and the spectra were measured by a Magnettech ESR5000 spectrometer. Considering that TEMPO has signal on EPR spectrum, the attenuation and recovery of the TEMPO signal on EPR spectrum was used to indicate the generation and transformation of $TEMPO^+$. NHPI, on the other side, has no signal on EPR spectrum. Thus, DMPO, a spin trapping agent that can trap PINO, was used to indicate the transformation between NHPI and PINO. In the first experimental group, TEMPO was dissolved in DI water and subjected to UV or dark treatments to explore the stability of TEMPO/$TEMPO^+$ cycle (TEMPO cannot be mineralized by UV irradiation), and the transformation time from TEMPO to $TEMPO^+$ under sole UV irradiation. In the second experimental group, TEMPO was dissolved in NaOCl solution and subjected to UV or dark treatments to investigate the acceleration of transformation from TEMPO to $TEMPO^+$ by UV/Chlorine process. In the third experimental group, NHPI solution, NaOCl solution, and mixture of NaOCl with NHPI in the solvent of acetonitrile were subjected to UV or dark treatments. The results were compared to reveal the acceleration of transformation from NHPI to PINO by UV/Chlorine process.

All of the above experiments were conducted in triplicate, and the relative standard deviations of the three replicates were below 5%.

2.3. Analytical methods, second-order rate constants, steady-state concentrations of radicals, and their contributions to RBV photodegradation

The absorption spectra of RBV, TEMPO, and NHPI (SI Fig.S2) were measured using a UV–vis spectrophotometer (UV-1750, Shimadzu). Competition kinetic method was used for calculating second-order rate constants, which was detailed in SI Text S2. The method to estimate steady state concentrations of radicals and their contributions to RBV photodegradation were detailed in SI Text S3 and Text S4. The measurement methods of RBV and its degradation products, probe compounds for radicals, free chlorine concentration, water quality parameters, as well as the parameters for EPR measurement were detailed in SI Text S5.

2.4. Computational methods

The DFT calculation of RBV and its Triazole-Carboxyamide structure (TC, illustrated in Fig. S1) were conducted by the Gaussian 09 software with DFT module. The geometry optimization and energy estimation of RBV molecule was conducted by B3LYP method with 6–31 G basis set [29]. The Highest Occupied Molecular Orbital (HOMO) and Lowest Unoccupied Molecular Orbital (LUMO) were calculated on the 6–31 G basis set with SMD solvent (water) module [30]. Besides, the Fukui index of TC was calculated by the Multiwfn software based on the geometry optimization results [31].

Ecological Structure Activity Relationship (ECOSAR) was used to assess the acute toxicity and chronic toxicity of RBV and its degradation products to fish, daphnid, and green algae, according to their molecular structures [32].

3. Results and discussion

3.1. Second-order rate constants of RBV vs. reactive species

Radicals, such as HO• and RCSs (e.g., Cl•, $Cl_2^{\bullet-}$, and ClO•) that are generated in UV/Chlorine process, react with pollutants at different rates [33,34]. Thus, the second order rate constants of RBV vs. HO•, RCSs, and HOCl were determined and the results are shown in Fig.S3-S7 and Table 1.

According to Table 1, the second order rate constant of HO• vs. RBV ($k_{HO\cdot-RBV}$) is 1.27×10^9 $M^{-1}{\cdot}s^{-1}$. The second order rate constants of Cl• and ClO• vs. RBV ($k_{Cl\cdot-RBV}$ and $k_{ClO\cdot-RBV}$) are 5.30×10^8 $M^{-1}{\cdot}s^{-1}$ and 5.58×10^7 $M^{-1}{\cdot}s^{-1}$, respectively. The second order rate constant of $Cl_2^{\bullet-}$ vs. RBV ($k_{Cl_2\cdot^- -RBV}$) is 2.83×10^5 $M^{-1}{\cdot}s^{-1}$, indicating that this radical will affect the degradation of RBV only when the steady state concentration of $Cl_2^{\bullet-}$ is high [33,35–37]. Besides, the second order rate constant of RBV vs. free chlorine ($k_{HOCl-RBV}$) is 4.0 $M^{-1}{\cdot}s^{-1}$.

3.2. Concentration-dependent effect of redox mediators on the degradation of RBV by UV/Chlorine process

The effect of TEMPO and NHPI concentrations on RBV photodegradation by UV/Chlorine process is illustrated in Fig. 1. As the concentration of TEMPO increased from 0 to 0.1 μM, the pseudo 1st order rate constant of RBV ($k_{obs-RBV}$) increased from 1.97×10^{-4} s^{-1} to 2.57×10^{-4} s^{-1} by 30%, indicating that low concentration of TEMPO could promote the degradation of RBV by UV/Chlorine process. Nonetheless, $k_{obs-RBV}$ decreased from 2.57×10^{-4} s^{-1} to 1.94×10^{-4} s^{-1} when the concentration of TEMPO increased from 0.1 μM to 0.2 μM, suggesting that high concentration of TEMPO inhibited the degradation of RBV by this process. Thus, TEMPO plays a dual role in RBV degradation by UV/Chlorine process, depending on its concentration. This phenomenon may be attributed to two mechanisms. One mechanism is that TEMPO tends to be oxidized into $TEMPO^+$ by the radicals generated in UV/Chlorine process, which could oxidize the secondary alcohol hydroxyl group into carbonyl group to promote the degradation of RBV [19,38]. The other mechanism is that high concentration of TEMPO could act as a radical scavenger, which consumes radicals generated in UV/Chlorine process and inhibits the degradation of RBV [12,39,40].

Similarly, $k_{obs-RBV}$ increased from 1.97×10^{-4} s^{-1} to 3.0×10^{-4} s^{-1}, and then decreased to 2.68×10^{-4} s^{-1} when the concentration of NHPI increased from 0 μM to 5 μM. The maximum $k_{obs-RBV}$ appeared at the NHPI concentration of 1 μM, which was 52% higher than that observed in UV/Chlorine process without NHPI, illustrating that low concentration of NHPI could strongly promote the degradation of RBV by UV/Chlorine process. This may be attributed to the low bond energy of O-H (88 $kcal{\cdot}mol^{-1}$) in the N-OH group of NHPI, which could be cleaved by UV photons. Then, NHPI is transformed into PINO, a kind of reactive intermediate that could not only promote the generation of radicals by UV/Chlorine process, but also degrade RBV as an oxidant. However, high concentration of NHPI (> 1 μM) could scavenge radicals, which inhibits the RBV degradation and reduces $k_{obs-RBV}$ [19,41–43].

As a redox mediator, NHPI could be oxidized into PINO by reactive

Table 1
Second-Order Rate Constants of RBVvs. HO·, Cl·, $Cl_2^{\bullet-}$, ClO·and HOCl ($M^{-1}{\cdot}s^{-1}$).

Rate constants	$k_{HO\cdot-RBV}$	$k_{Cl\cdot-RBV}$	$k_{ClO\cdot-RBV}$	$k_{Cl_2\cdot^- -RBV}$	$k_{HOCl-RBV}$
value	1.27×10^9	5.30×10^8	5.58×10^7	2.83×10^5	4.0

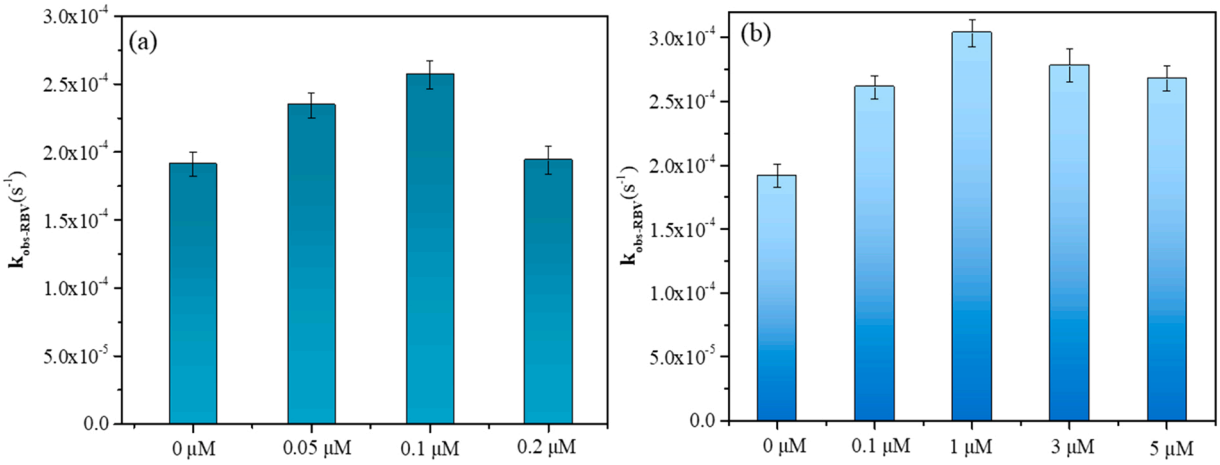

Fig. 1. (a) Effect of TEMPO concentrations on the pseudo 1st order degradation rate constants of RBV; (b) Effect of NHPI concentrations on the pseudo 1st order degradation rate constants of RBV (Condition: $[Chlorine]_0 = 42$ μM; $[RBV]_0 = 10$ mg·L^{-1}; $[TEMPO]_0 = 0, 0.05, 0.1, 0.2$ μM; $[NHPI]_0 = 0, 0.1, 1, 3, 5$ μM; pH = 7.0; Temperature = 25 °C).

intermediates such as HO•. When NHPI is at low concentration, all of the molecules could be transformed into PINO to enhance RBV degradation. However, as the concentration of NHPI increases, NHPI molecules are partially oxidized into PINO, and the residual NHPI molecules could inhibit the degradation of RBV by two mechanisms. One mechanism is that the residual NHPI could react with free chlorine to generate PINO. Although PINO is produced, the efficiency of PINO generation is too low. In addition, free chlorine, as the precursor of reactive oxygen species (ROSs) and RCSs, is consumed by NHPI in this process, resulting in the reduced generation of free radicals, which eventually inhibits the enhancement of NHPI on RBV degradation by UV/Chlorine process. This conclusion was also confirmed by the results of EPR analyses in this study. The other mechanism is that the residual NHPI would have a light shielding effect on free chlorine. Given that the molar absorption coefficient of NHPI (292 M^{-1}•s^{-1}) is greater than that of free chlorine (HOCl: 59 M^{-1}•s^{-1} and OCl^-: 66 M^{-1}•s^{-1}), the residual NHPI would compete with free chlorine for UV photons, which would lower the exciting efficiency of free chlorine and finally inhibit the RBV photodegradation by UV/Chlorine/NHPI process [33,44].

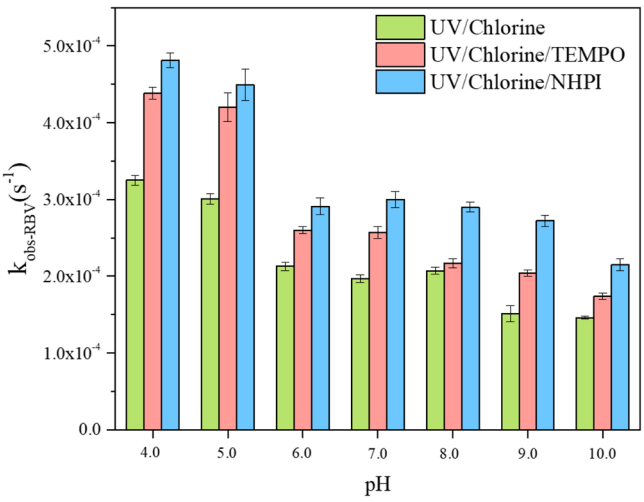

Fig. 2. Effect of pH on the degradation of RBV in UV/Chlorine in the absence or presence of redox mediators ($[RBV]_0 = 10$ mg·L^{-1}, $[Chlorine]_0 = 42$ μM, $[TEMPO]_0 = 0.1$ μM, $[NHPI]_0 = 1$ μM, pH = 4.0–10.0, Temperature = 25 °C).

3.3. Factors affecting the RBV degradation by UV/Chlorine processes with and without redox mediators

The effects of pH (4.0–10.0) on RBV photodegradation by UV/Chlorine process with and without redox mediators are depicted in Fig. 2. The results demonstrate that the $k_{obs-RBV}$ by UV/Chlorine process without redox mediators generally decreases with the increase of pH, except for pH = 8.0. This is because that free chlorine tends to exist in the form of of OCl^- rather than HOCl in alkaline solution, leading to low quantum yields of HO• and Cl• under UV irradiation, which weakens the degradation of RBV [45].

Nonetheless, the $k_{obs-RBV}$ by UV/Chlorine process is higher at pH = 8.0 than those at pH = 7.0 and 9.0. To explain this phenomenon, the RBV molecule was analyzed. It was found that the hydrolysis of carboxyamide structure in RBV molecule could increase the electron cloud intensity of the triazole structure connected to it. The triazole structure could be readily attacked by radicals, which would accelerate the disintegration of TC structure in RBV molecule. Thus, the increase of $k_{obs-RBV}$ by UV/Chlorine process might be attributed to the hydrolysis of carboxyamide structure in RBV molecules when pH increases from 7.0 to 8.0. In order to further verify this deduction, the HOMO orbital of TC structure was calculated by Gaussian 09, which is shown in Fig. 3. The results demonstrate that the hydrolysis in alkaline solution could increase the electron cloud intensities of N10, N16, and N17 atoms in RBV molecule, which would increase the reactivities of radicals vs. triazole structure in RBV molecule and promote the degradation of RBV.

In addition, the Fukui index of TC structure was calculated, which demonstrated that the hydrolysis of carboxyamide structure would increase the electrophilic Fukui indices (*f*-) of N10, N16 and N17 atoms in RBV molecule. Thus, the electron cloud intensity of TC in RBV molecule would increase as the hydrolysis of carboxyamide structure, which could promote the degradation efficiency of RBV. The steady-state concentration of HO• will slightly decrease as pH increases from 7.0 to 8.0, but is still sufficient to support the degradation of RBV. Therefore, $k_{obs-RBV}$ at pH = 8.0 is higher than that at pH = 7.0.

However, the steady-state concentration of radicals would experience a sharply decrease as the pH increases from 8.0 to 9.0 and 10.0. In this pH range, the enhancement of RBV degradation by the hydrolysis of carboxyamide structure will not be able to compensate the decrease of the steady-state concentrations of radicals, which will finally lead to the decrease of $k_{obs-RBV}$ [46,47]. A similar finding was also reported in a previous study on the oxidation of 2,4-dichlorophenol and triclosan by potassium permanganate [48–50].

When TEMPO was added into UV/Chlorine process, the $k_{obs-RBV}$ increased to 4.38×10^{-4} s^{-1}, 4.20×10^{-4} s^{-1}, $2.6\ 0 \times 10^{-4}$ s^{-1},

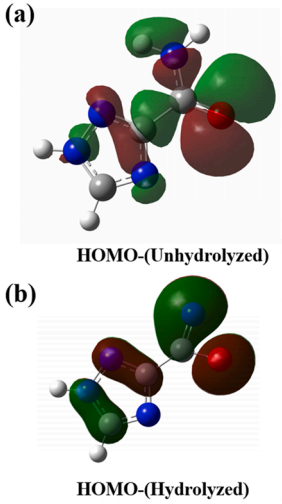

No	(Atom)	Charge(0) (e/Å3)	Charge(+1) (e/Å3)	Charge(-1) (e/Å3)	*f*-	*f*+
1	10(N)	-0.0007	-0.0908	0.055	0.0557	0.0901
2	11(C)	0.0606	-0.0378	0.1231	0.0625	0.0983
3	12(N)	-0.1824	-0.2482	-0.117	0.0654	0.0657
4	13(C)	0.0626	-0.0385	0.0851	0.0225	0.1011
5	14(C)	0.1591	0.0575	0.2469	0.0877	0.1016
6	15(O)	-0.304	-0.4394	0.0565	0.3605	0.1354
7	16(N)	-0.1475	-0.2119	-0.0486	0.0989	0.0643
8	17(N)	-0.1508	-0.3012	-0.083	0.0677	0.1504

No	(Atom)	Charge(0) (e/Å3)	Charge(+1) (e/Å3)	Charge(-1) (e/Å3)	*f*-	*f*+
1	10(N)	0.0152	-0.0329	0.079	0.0638	0.0481
2	11(C)	0.0711	0.0158	0.1452	0.0741	0.0553
3	12(N)	-0.1765	-0.2096	-0.1326	0.0439	0.0331
4	13(C)	0.0742	0.0635	0.0991	0.0249	0.0108
5	14(C)	0.1466	0.0163	0.2423	0.0957	0.1303
6	15(O)	-0.1632	-0.4469	0.0754	0.2386	0.2837
7	16(N)	-0.0995	-0.4093	0.2033	0.3028	0.3098
8	17(N)	-0.1221	-0.1784	-0.0434	0.0787	0.0564

Fig. 3. (a) HOMO orbital distribution and corresponding Fukui index of TC structure when carboxyamide is not hydrolyzed, (b) HOMO orbital distribution and corresponding Fukui index of TC structure after carboxyamide is hydrolyzed.

2.57×10^{-4} s^{-1}, 2.17×10^{-4} s^{-1}, 2.04×10^{-4} s^{-1}, and 1.74×10^{-4} s^{-1} at pH = 4.0, 5.0, 6.0, 7.0, 8.0, 9.0, and 10.0, respectively, demonstrating that the $k_{obs-RBV}$ by UV/Chlorine/TEMPO process in acidic solutions is higher than those in neutral and alkaline solutions. This might be explained by the fact that free chlorine tends to exist in the form of HOCl rather than OCl^- in acidic solution, leading to high quantum yields of HO• and Cl• under UV irradiation to accelerate the TEMPO/$TEMPO^+$ cycle, thereby promote the degradation of RBV.$k_{obs-RBV}$ increased in varying degrees after adding TEMPO in UV/Chlorine process in all seven pH solutions, and most of the increase rate of $k_{obs-RBV}$ from UV/Chlorine process to UV/Chlorine/TEMPO process were over 30% except that in the solutions of pH = 6.0 and 8.0.

At pH = 6.0, there was a 22% increase of $k_{obs-RBV}$ from changing UV/Chlorine process to UV/Chlorine/TEMPO process, which was lower than those increases observed at pH = 5.0 and 7.0 (40% and 31%, respectively). This was because that the increase of HO• was not strong enough to promote RBV degradation as pH decreased from 7.0 to 6.0. In this pH range, the inhibition on $TEMPO^+$ generation by proton was amplified, which resulted in a poor enhancement of TEMPO on RBV degradation by UV/Chlorine process [51,52].

At pH = 8.0, $k_{obs-RBV}$ by UV/Chlorine/TEMPO process was 4.8% higher than that by UV/Chlorine process, which was lower than those at pH = 7.0 (31%) and 9.0 (35%). On one hand, the hydrolysis of carboxyamide group in RBV molecule increased the electron cloud intensity of TC structure, which promoted the vulnerability of TC structure to radicals, resulting in the increase of $k_{obs-RBV}$. On the other hand, the yield of HO• was low in alkaline solution, which inhibited the generation of $TEMPO^+$. Meanwhile, the hydrolysis of carboxyamide group in RBV molecule increased the electron cloud intensity of TC structure of RBV, which promoted the attack of radicals to TC structure, resulting in a high value of $k_{obs-RBV}$in UV/Chlorine process without TEMPO. Thus, the increase rate of $k_{obs-RBV}$ was small in UV/Chlorine/TEMPO because it increased from a relatively high value of $k_{obs-RBV}$in UV/Chlorine process.

When NHPI was added into UV/Chlorine process, $k_{obs-RBV}$ increased to 4.81×10^{-4} s^{-1}, 4.49×10^{-4} s^{-1}, 2.91×10^{-4} s^{-1}, 3.00×10^{-4} s^{-1}, 2.90×10^{-4} s^{-1}, 2.72×10^{-4} s^{-1}, and 2.15×10^{-4} s^{-1} at pH = 4.0, 5.0, 6.0, 7.0, 8.0, 9.0, and 10.0, respectively, indicating that the enhancement of NHPI on RBV degradation by UV/Chlorine process was affected by the pH of solution. The obtained $k_{obs-RBV}$ values were generally higher in acidic solutions than those in neutral and alkaline solutions, which were caused by the high yields of radicals in acidic solution that promoted the transformation of NHPI to PINO. Besides, the enhancement of NHPI to RBV in UV/Chlorine process varied with acid-base properties of reactive solution, and most of the increase rate of $k_{obs-RBV}$ from UV/Chlorine process to UV/Chlorine/NHPI process were over 40% except that in the solutions of pH = 6.0.

At pH = 6.0, $k_{obs-RBV}$ was lower than that at pH = 7.0 by UV/Chlorine/NHPI process. This was because that there were at least two pathways to generate PINO in UV/Chlorine/NHPI process. In one pathway, PINO was generated from the oxidation of NHPI by free chlorine and radicals. In the other pathway, the formation of hydrogen-bond between NHPI and RBV molecules would also promote the generation of PINO. However, the concentration of protons increases with the decrease of pH. Proton will be close to the triazole (TC) structure with high electron cloud intensity in RBV molecule, and occupy the active site where is easy to form hydrogen bond. Thus, hydrogen bond between NHPI and RBV was weakened. Meanwhile, the generation of radicals by UV/Chlorine process in weak acidic solution was similar to that in neutral solution, which was not enough to offset the negative impact of reduction on PINO generation, leading to a low $k_{obs-RBV}$ at pH = 6.0 [51,52]. This was also the reason why the $k_{obs-RBV}$ increased 37% from changing UV/Chlorine process to UV/Chlorine/NHPI process at pH = 6.0, which was lower than those at pH = 5.0 and 7.0 (49% and 52%,

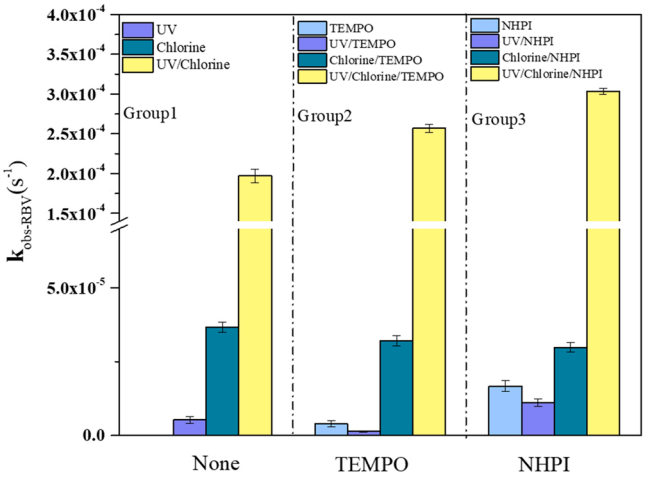

Fig. 4. Pseudo 1st order degradation rate constants of RBV in different processes ($[RBV]_0$ = 10 mg·L^{-1}, $[Chlorine]_0$ = 42 μM, $[TEMPO]_0$ = 0.1 μM, $[NHPI]_0$ = 1 μM, pH = 7.0, Temperature = 25 °C).

respectively).

Fig. 4 depicted the $k_{obs-RBV}$ values obtained from different processes (i.e., UV only, free chlorine only, UV with redox mediators, free chlorine with redox mediators, and UV/Chlorine with redox mediators). Their time-dependent degradations are shown in Fig.S10. According to Fig. 4, the $k_{obs-RBV}$ by UV/Chlorine process is 1.97×10^{-4} s^{-1}, which is 5.4 times higher than that by free chlorine (42.0 μM as Cl_2) only process, and 37% higher than that by UV only process. However, the $k_{obs-RBV}$ by UV/Chlorine/TEMPO process is 1.3 times higher than that by UV/Chlorine process. Additionally, the $k_{obs-RBV}$ by UV/Chlorine/NHPI process is 1.52 times higher than that by UV/Chlorine process. These results demonstrate that redox mediators can strongly promote RBV degradation by UV/Chlorine process. Of note, redox mediators could inhibit RBV degradation by free chlorine (42.0 μM as Cl_2) only process. Their enhancements on RBV degradation by UV only process are also limited. These findings indicate that redox mediators, under radical-limited conditions, would inhibit RBV oxidation by chlorine and could not enhance the photolysis of RBV. Thus, it can be inferred that the enhancement of redox mediators on RBV degradation is mainly attributed to the radicals generated by UV/Chlorine process, whose detailed mechanisms need to be further investigated on the basis of radical measurement.

3.4. Contributions of different radicals toward RBV degradation and the radical-dependent oxidations of redox mediators

The steady state concentrations of radicals ($[HO\bullet]_{ss}$, $[Cl\bullet]_{ss}$, $[Cl_2^{\bullet-}]_{ss}$, and $[ClO\bullet]_{ss}$) generated by UV/Chlorine, UV/Chlorine/TEMPO, and UV/Chlorine/NHPI processes were estimated according to the method described in SI Text S3. The results are summarized in Table 2 and Fig. S12.

In Table 2, the influences of processes on the $[HO\bullet]_{ss}$, $[Cl\bullet]_{ss}$, $[Cl_2^{\bullet-}]_{ss}$, and $[ClO\bullet]_{ss}$ are limited. Nevertheless, $[ClO\bullet]_{ss}$ decreased to 0 M in UV/Chlorine/TEMPO process and decreased by 82.15% in UV/Chlorine/NHPI process comparing to that in UV/Chlorine process, indicating that redox mediators could inhibit the generation of ClO• but rarely affect the generations of HO•, Cl•, and $Cl_2^{\bullet-}$. Since free chlorine is one of the precursors of ClO•, it can be inferred that the degradation rate of free chlorine will reduce when redox mediators are added into UV/Chlorine process. To test this inference, the concentration of free chlorine was measured during the UV/Chlorine processes with and without redox mediators. The results (Fig.S15) confirmed the inference that redox mediators could inhibit or even stop the generation of ClO• by hindering the reaction between free chlorine vs. HO• and Cl•.

Fig. 5 depicts the contributions of UV, free chlorine, and various radicals to the $k_{obs-RBV}$ by different processes, which were calculated by Eq. (S15)-(S19). The results indicate that the UV/chlorine process would strongly promote the degradation of RBV comparing to UV only or free chlorine only processes. Additionally, HO• was the major contributor for the degradation of RBV in this process, which accounted for 67% of RBV removal. The rest of RBV removal was accomplished by free chlorine and other RCSs.

When TEMPO was added into UV/Chlorine process, the $k_{obs-RBV}$ increased from 1.97×10^{-4} s^{-1} to 2.57×10^{-4} s^{-1}, and HO• still dominated the degradation of RBV with a contribution of 50%. Meanwhile, the contributions of Cl• and $Cl_2^{\bullet-}$ toward $k_{obs-RBV}$ did not change

Table 2
Steady-state concentrations of HO• and RCSs.

Conditions	$[HO\bullet]_{ss}$/M	$[Cl\bullet]_{ss}$/M	$[ClO\bullet]_{ss}$/M	$[Cl_2^{\bullet-}]_{ss}$/M
UV/Chlorine	1.02×10^{-13}	3.42×10^{-14}	3.44×10^{-13}	3.11×10^{-11}
UV/Chlorine/TEMPO	1.02×10^{-13}	3.27×10^{-14}	0	3.38×10^{-11}
UV/Chlorine/NHPI	1.01×10^{-13}	3.36×10^{-14}	6.14×10^{-14}	3.20×10^{-11}

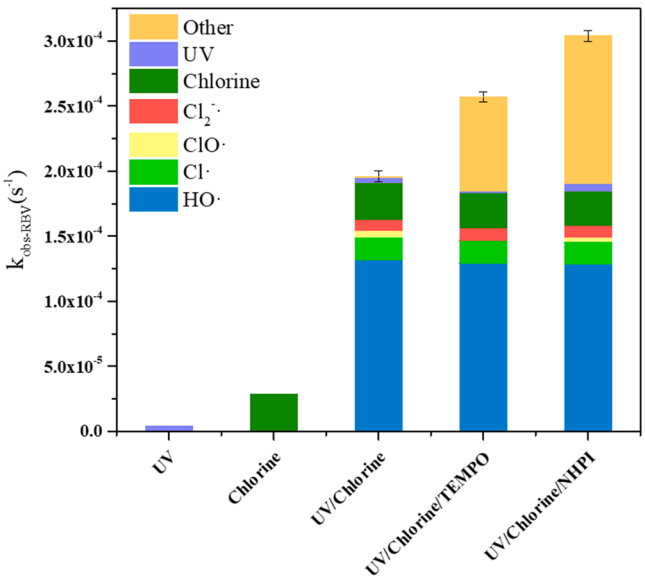

Fig. 5. Pseudo 1st order rate constants of RBV in UV_{254} only, NaOCl only, UV_{254}/Chlorine, UV_{254}/Chlorine/TEMPO and UV_{254}/Chlorine/NHPI process, and the contributions of UV, free chlorine and reactive intermediates toward $k_{obs-RBV}$.

significantly but the contribution of ClO• decreased to 0%. Moreover, the contribution of unknown reactive intermediates toward RBV degradation increased from 0.38% to 28%. Therefore, it could be inferred that TEMPO was transformed into $TEMPO^+$ by UV/Chlorine process, which could oxidize secondary hydroxyl group into carbonyl group (see Eq. (1)). After oxidation, $TEMPO^+$ was reduced into TEMPOH, which is unstable and could be immediately transformed into TEMPO to take part in another TEMPO/$TEMPO^+$ cycle (as shown in Fig. S13) [38,53].

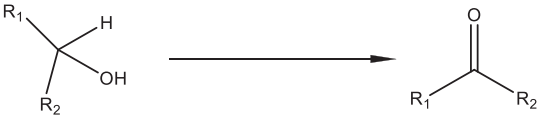

(1)

Similar phenomenon was also observed in UV/Chlorine/NHPI process. When NHPI was added, the $k_{obs-RBV}$ increased from 1.97×10^{-4} s^{-1} to 3.0×10^{-4} s^{-1}, in which 42%was contributed by HO•. The contributions of Cl• and $Cl_2^{\bullet-}$ toward $k_{obs-RBV}$ did not change significantly but the contribution of ClO• decreased from 2.4% to 1.1%, indicating that NHPI could inhibit but not stop the generation of ClO•. Nonetheless, the contribution of unknown reactive intermediates toward RBV photodegradation increased from 0.38% to 37.4%. This may be attributed to the enhancement of PINO (a reactive intermediate, derived from NHPI) on RBV photodegradation. The hydrogen connected to the O12 on NHPI molecule (Fig.S11) can form hydrogen bond with the N12 on RBV molecule, which promotes the generation of PINO by facilitating the N-O12 bond break in NHPI molecules. At the same time, free chlorine could also promote the yield of PINO by facilitating the N-O12 bond break. PINO is a kind of oxidant that can extract the hydrogen from the secondary carbon on RBV molecule. Then, RBV is transformed into its corresponding carbonaceous radical (R-R•-R). Meanwhile, PINO can be reduced to NHPI. Thus, the NHPI-PINO cycle is formed as shown in Fig. S14 and Eq. (2), which is deeply depended on radicals and oxidants [23, 43,53].

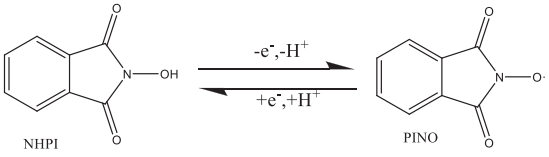

(2)

To reveal the role of unknown reactive intermediates played in RBV photodegradation, TBA scavenging experiments were conducted for UV/Chlorine, UV/Chlorine/TEMPO, and UV/Chlorine/NHPI processes. The second order rate constants of different radicals vs. TBA were summarized in Table S2. The $k_{obs-RBV}$with and without radicals scavenging by TBA were determined for the three processes, which are depicted in Fig. 6. With the addition of TBA, the $k_{obs-RBV}$ by UV/Chlorine process decreased 63% from 1.97×10^{-4} s^{-1} to 0.72×10^{-4} s^{-1}, indicating that the radicals of HO•, Cl•, ClO• contributed approximately 63% (Eq. (S20)) to the RBV photodegradation, which is slightly lower than the contribution by HO• according to Eq. (S16)-(S19). This may be explained by that a small amount of H_2O_2 could be generated during the scavenging of HO• by TBA, which could oxidize RBV and impact the results of scavenging experiment [54].

Nevertheless, the $k_{obs-RBV}$ by UV/Chlorine/TEMPO and UV/Chlorine/NHPI processes decreased 66% (from 2.57×10^{-4} s^{-1} to 0.88×10^{-4} s^{-1}) and 72% (from 3.0×10^{-4} s^{-1} to 0.85×10^{-4} s^{-1}) with the addition of TBA, respectively. In these two processes, the contributions of the radicals scavenged by TBA were far greater than that of HO• to RBV degradation, indicating that $TEMPO^+$ and PINO were also scavenged by TBA since the sum of contributions by RCSs towards RBV degradation was below 5%.

It is worth to mention that the $k_{obs-RBV}$ by UV/Chlorine, UV/Chlorine/TEMPO, and UV/Chlorine/NHPI processes with TBA additions were approximately equal to the sum of contributions by free chlorine and UV toward $k_{obs-RBV}$, demonstrating that the contribution of unknow reactive intermediates to RBV photodegradation decreased to 0% in UV/Chlorine/TEMPO and UV/Chlorine/NHPI processes with TBA additions, which also indicated that the existence of radicals (e.g., HO•, Cl•, and ClO•) was necessary for TEMPO and NHPI activations. Therefore, the enhancement of redox mediators on RBV degradation by UV/Chlorine process is mainly attributed to the reactive intermediates derived from redox mediators, whereas the enhanced generation of radicals by redox mediators (electron shuttle) has less contribution.

In order to further explore the roles of $TEMPO^+$ and PINO in RBV degradation by UV/Chlorine process with redox mediators, EPR spectra of them were identified to elucidate the enhancement mechanisms. The EPR signals of TEMPO in DI water are depicted in Fig. 7(a). The TEMPO signal in EPR spectrum was sharply attenuated after 5 min of UV irradiation, followed by a recover after 1.5 h of dark treatment, indicating that TEMPO was transformed into $TEMPO^+$ and TEMPOH under UV irradiation, which were unstable and transformed back to TEMPO in darkness [55].

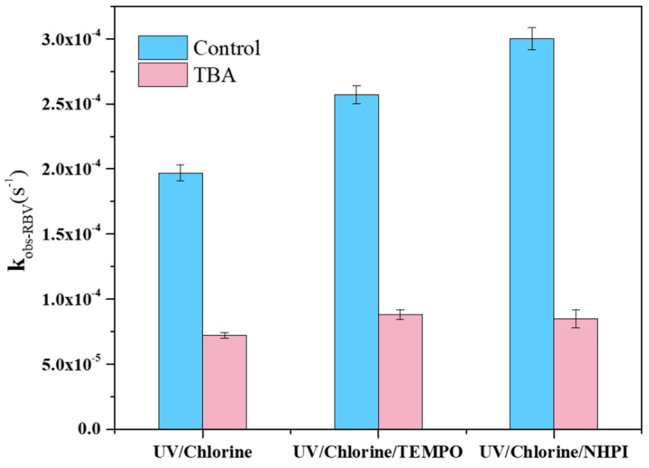

Fig. 6. Pseudo 1st order rate constants of RBV in UV/Chlorine process in the absence and presence of TBA solution. Control group means RBV degradation in UV/Chlorine process without TBA. TBA group means RBV degradation in UV/Chlorine process with TBA as a radical scavenger. ($[RBV]_0$ = 10 mg·L^{-1}, $[Cholrine]_0$ = 42 μM, TBA = 10 mM, pH = 7.0, Temperature = 25 °C).

Fig. 7(b) shows the EPR signals of TEMPO in NaOCl solution. There was no change on the EPR signal of TEMPO after 1.5 h of dark treatment, demonstrating that NaOCl could not transform TEMPO into $TEMPO^+$. However, the EPR signal of TEMPO attenuated rapidly after 2 s of UV irradiation, and disappeared after 10 s of UV irradiation, indicating that the UV/Chlorine process could significantly accelerate the transformation of TEMPO, which was faster than sole UV irradiation. After UV irradiation, the EPR signal of TEMPO recovered after a 40 min of dark treatment, suggesting that TEMPO was not decomposed but transformed into $TEMPO^+$/TEMPOH, which was transformed back to TEMPO in darkness [55]. These results confirmed that the enhanced RBV degradation by UV/Chlorine process was attributed to the $TEMPO^+$ transformed from TEMPO, and the radicals generated by UV/Chlorine process could significantly accelerate this transformation.

Likewise, PINO was detected by EPR when the solvent DI water was replaced with acetonitrile to prolong radical life [56]. According to Fig. 7(c), the EPR spectra of NHPI were not affected by sole UV irradiation, indicating that UV irradiation without NaOCl could not transform NHPI into PINO. Additionally, the NaOCl did not have EPR signal, whereas the NaOCl solution showed EPR signal after UV irradiation, which was caused by RCSs and ROSs. For NaOCl and NHPI mixture, weak EPR signal that is different from the signal of UV irradiated NaOCl solution was detected, which belonged to PINO [57]. This result suggested that the efficiency of PINO generation from the reaction of NHPI vs. free chlorine was very low. When the NaOCl and NHPI mixture solution was irradiated by UV light, the EPR signal of PINO was strongly enhanced, indicating that the radicals generated by UV/Chlorine process greatly accelerated the transformation from NHPI to PINO.

3.5. *Effect of water matrix on the enhancement of RBV degradation by UV/Chlorine process with redox mediators*

SRNOM from International Humic Substances Society (IHSS) was widely used as the standard sample of DOM to study its effect on pollutants degradation in advanced oxidation processes. Besides, HCO_3^- and Cl^- were the common anions in water matrix of real surface water. Thus, SRNOM, HCO_3^-, and Cl^- were chosen as common water quality parameters to study the effect of water matrix on the degradation of RBV by UV/Chlorine, UV/Chlorine/TEMPO, and UV/Chlorine/NHPI processes [58].

As shown in Fig. 8(a), the $k_{obs-RBV}$ by UV/Chlorine process decreased from 1.97×10^{-4} s^{-1} to 7.72×10^{-5} s^{-1} as the SRNOM concentration increased from 0 mgC•L^{-1} to 10 mgC•L^{-1}. As the concentration of SRNOM increased from 0 mgC•L^{-1} to 10 mgC•L^{-1}, $k_{obs-RBV}$ decreased from 2.57×10^{-4} s^{-1} to 9.43×10^{-5} s^{-1} and from 3.00×10^{-4} s^{-1} to 1.35×10^{-5} s^{-4} when TEMPO and NHPI were added into the UV/Chlorine process, respectively. This could be attributed to two mechanisms. One mechanism is that DOM could interfere with the photolysis of chlorine by inner filter effect, which would inhibit the generation of radicals by UV/Chlorine process [59]. The other mechanism is that SRNOM could compete with RBV for radicals and oxidative species (e.g., HO•, RCSs, $TEMPO^+$ and PINO) in the UV/chlorine system [38,60]. Therefore, the enhancement on RBV degradation by UV/Chlorine/Redox mediator process was weakened as the SRNOM concentration increased.

HCO_3^- and CO_3^{2-} could be converted into each other. However, the primary existing form was HCO_3^- rather than CO_3^{2-} in neutral solution. HCO_3^- could compete with RBV for OH• and Cl• due to their high reaction rate constants with OH• and Cl•, which would cause the reduction on $k_{obs-RBV}$ as depicted in Eqs. (3) - (5) [33,61]. Considering that the concentration of HCO_3^- in actual water is in the range of 0.3–3.0 mM, the HCO_3^- concentrations of 0, 0.5, 1.0, 3.0 mM were selected to further evaluate its effect on RBV photodegradation by UV/Chlorine, UV/Chlorine/TEMPO and UV/Chlorine/NHPI processes.

$$HO\cdot + HCO_3^- \rightarrow H_2O + CO_3^{\cdot -}, \mathrm{k} = 8.5 \times 10^6 M^{-1}s^{-1} \quad (3)$$

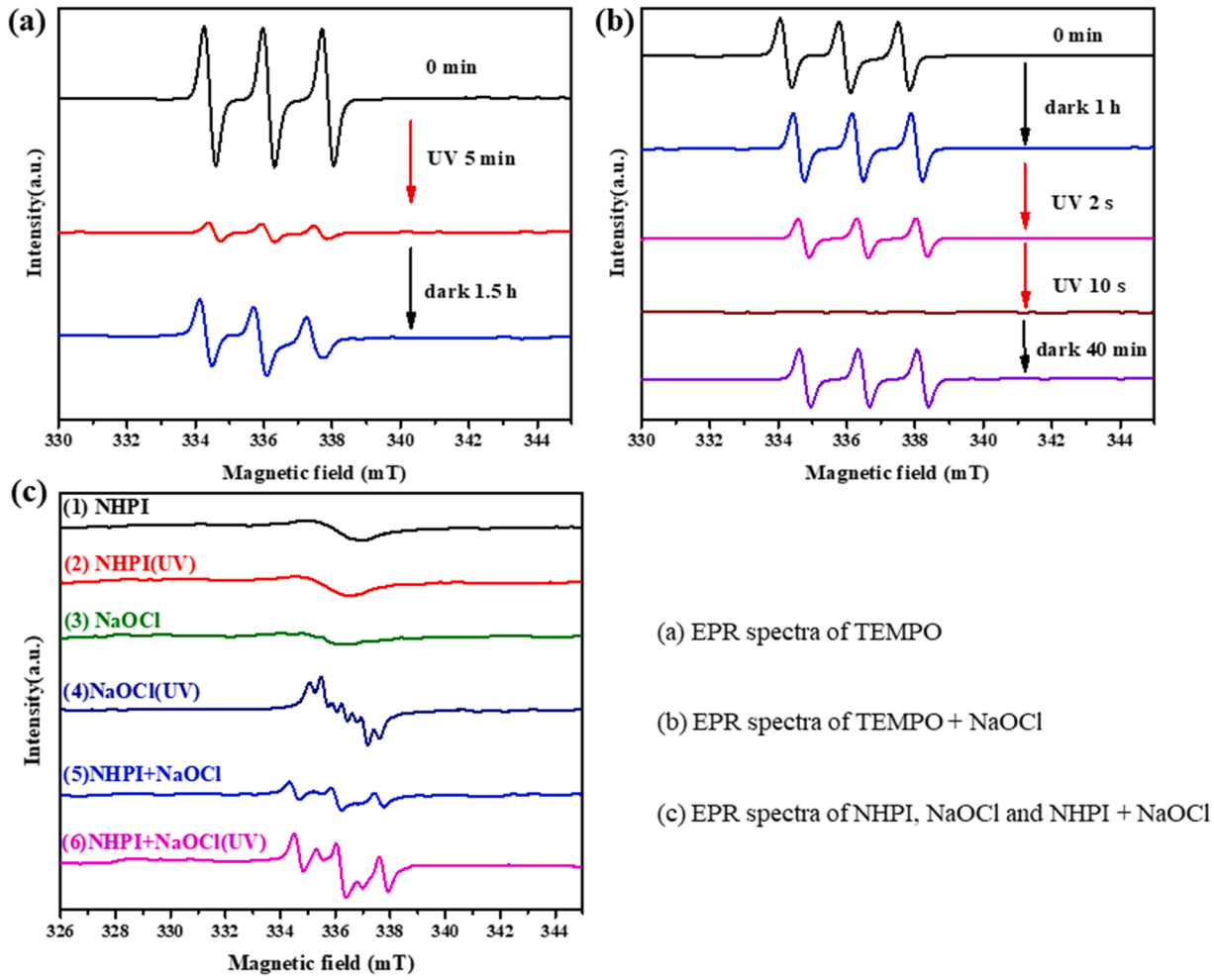

Fig. 7. EPR spectra. (a) TEMPO solution; (b) NaOCl/TEMPO solution; (c):(1) NHPI solution, (2) NHPI solution after 1 min UV light irradiation, (3) NaOCl solution, (4) NaOCl solution after 1 min UV light irradiation, (5) NaOCl/NHPI, (6) NaOCl/NHPI after 1 min UV light irradiation. Conditions: Irradiation light source is UV lamp with wavelength of 254 nm; NaOCl: 4.2 mM; TEMPO: 10 μM; NHPI: 100 μM. Solvent of (a) and (b) is deionized water, and solvent of (c) is acetonitrile.

$$HO\cdot + CO_3^{2-} \rightarrow CO_3^{\cdot -} + OH^-, \mathrm{k} = 3.9 \times 10^8 M^{-1}\mathrm{s}^{-1} \quad (4)$$

$$Cl\cdot + HCO_3^- \rightarrow H_2O + CO_3^{\cdot -}, \mathrm{k} = 2.2 \times 10^8 M^{-1}\mathrm{s}^{-1} \quad (5)$$

The effect of HCO_3^- concentration on degradation of RBV by UV/Chlorine process is depicted in Fig. 8(b). The $k_{obs-RBV}$ by UV/Chlorine process decreased from 1.97×10^{-4} s^{-1} to 1.70×10^{-4} s^{-1} as the concentration of HCO_3^- increased from 0 mM to 3.0 mM. This was because that HCO_3^- consumed HO• and Cl• to produce $CO_3^{\bullet -}$, which is less reactive than HO• and Cl• [61]. Meanwhile, as the HCO_3^- concentration increased from 0 mM to 3 mM, the $k_{obs-RBV}$ decreased from 2.57×10^{-4} s^{-1} to 1.77×10^{-4} s^{-1} and from 3.00×10^{-4} s^{-1} to 1.70×10^{-4} s^{-1} when TEMPO and NHPI were added into UV/Chlorine process, respectively. These results confirmed that the consumption of HO• would decrease the enhancement of TEMPO and NHPI on RBV photodegradation by UV/chlorine process.

Effect of Cl^- concentration on RBV degradation by UV/Chlorine process with and without redox mediators is illustrated in Fig. 8(c). The Cl^- concentrations of 0, 5, 10, 20 mM were selected because the concentration of Cl^- in actual surface water is in the range of 0–20 mM [58, 62]. According to Fig. 8(c), the $k_{obs-RBV}$ by UV/Chlorine process decreased from 1.97×10^{-4} s^{-1} to 1.51×10^{-4} s^{-1} as the concentration of Cl^- increased from 0 mM to 20 mM. This could be explained by that Cl^- could react with Cl• ($k_{Cl\bullet\text{-}RBV} = 5.30 \times 10^8$ $M^{-1}\bullet s^{-1}$) to form $Cl_2^{\bullet -}$ ($k_{Cl_2^{\bullet -}-RBV} = 2.83 \times 10^5$ $M^{-1}\bullet s^{-1}$), which is a weak reactive intermediate and thereby inhibit the degradation of RBV. Moreover, Cl^- could also react with HO• to generate Cl•, which would consume HO• and thus inhibited the degradation of RBV [63]. Besides, as the concentration of Cl^- increased from 0 mM to 20 mM, the $k_{obs-RBV}$ by UV/Chlorine process decreased from 2.57×10^{-4} s^{-1} to 1.58×10^{-4} s^{-1} and from 3.00×10^{-4} s^{-1} to 1.68×10^{-4} s^{-1} in the presence of TEMPO and NHPI, respectively. These results indicated that the enhancement of TEMPO and NHPI on RBV degradation by UV/Chlorine process was inhibited by Cl^-, which could be resulted from the consumption of HO• by Cl^- that led to less generations of $TEMPO^+$ and PINO.

The effects of the two redox mediators on RBV degradation by UV/Chlorine process were also examined in two actual water matrices, which were collected from reservoir (EW) and river (NW). The geographical sampling locations of these two actual surface waters are depicted in Fig.S42. The $k_{obs-RBV}$ by UV/Chlorine process with and without redox mediators were determined in two actual surface water matrices (Fig. 9). The $k_{obs-RBV}$ were 1.62×10^{-4} s^{-1} in river water and 1.85×10^{-4} s^{-1} in reservoir water, which were lower than that in DI water (1.97×10^{-4} s^{-1}), indicating that actual water matrix generally inhibits the degradation of RBV by UV/Chlorine process. The inhibition may be attributed to the presence of dissolved organic matter (DOM) in actual surface waters, which could weaken the RBV degradation by two mechanisms. One mechanism is that DOM could compete with HOCl for UV photons, which would decrease the yield of radicals in UV/Chlorine process. The other mechanism is that DOM is a radical quencher, which would scavenge the radicals and inhibit the degradation of RBV [64].

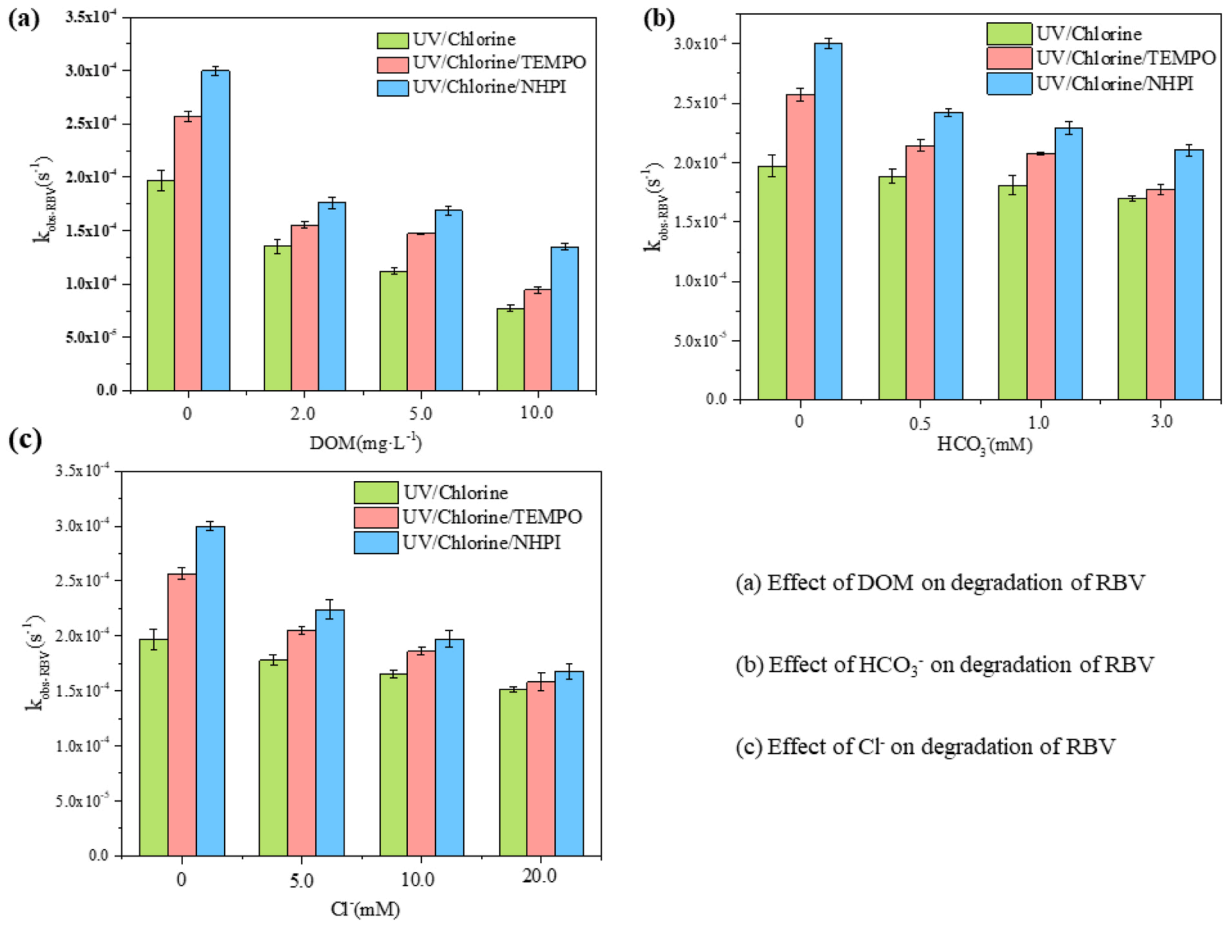

Fig. 8. Effect of DOM and two anions on pseudo 1st order degradation rate constants of RBV in UV/Chlorine process in the absence and presence of redox mediators (a) DOM, (b) HCO_3^-, (c) Cl^-. ([RBV]$_0$ = 10 mg·L^{-1}, [Chlorine]$_0$ = 42 μM, [TEMPO]$_0$ = 0.1 μM, [NHPI]$_0$ = 1 μM, pH = 7.0, Temperature = 25 °C).

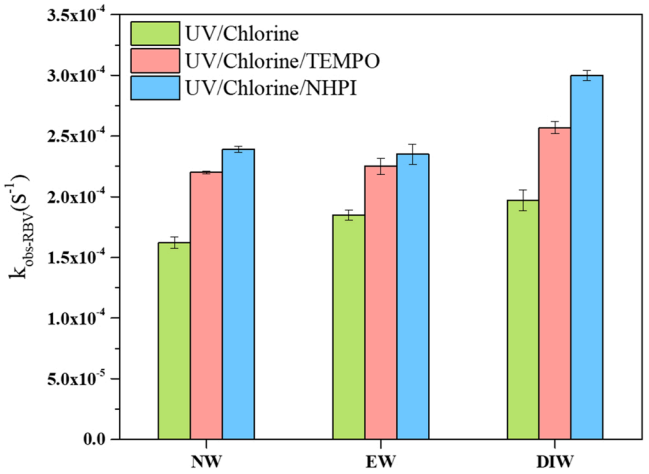

Fig. 9. Pseudo 1st order degradation rate constants of RBV in UV/Chlorine process in the absence and presence of redox mediators in two real surface water samples; NW referred to the water collected from Minjiang River; EW referred to the water collected from Tangban Reservoir; DIW referred to deionized water. ([RBV]$_0$ = 10 mg·L^{-1}, [Chlorine]$_0$ = 42 μM, [TEMPO]$_0$ = 0.1 μM, [NHPI]$_0$ = 1 μM, Temperature = 25 °C).

The UV absorbance at 355 nm (a(355)) commonly represent the abundance of DOM in actual water. In Table S1, a(355) values for river and reservoir water are 4.61 and 4.45, respectively, indicating that the abundance of DOM in river water was higher than that in reservoir water, which led to a lower $k_{obs-RBV}$ by UV/Chlorine process in river water.

Nevertheless, the $k_{obs-RBV}$ in river water increased by 27% (from 1.62 ×10^{-4} s^{-1} to 2.21 ×10^{-4} s^{-1}) and 32% (from 1.62 ×10^{-4} s^{-1} to 2.39 ×10^{-4} s^{-1}) when TEMPO and NHPI were added into the UV/Chlorine process, respectively. Similarly, the$k_{obs-RBV}$ in reservoir water increased by 18% (from 1.85 ×10^{-4} s^{-1} to 2.25 ×10^{-4} s^{-1}) and 27% (from 1.85 ×10^{-4} s^{-1} to 2.35 ×10^{-4} s^{-1}) when TEMPO and NHPI were added into the UV/Chlorine process, respectively. These results indicate that TEMPO and NHPI are able to enhance the RBV degradation by UV/Chlorine process in actual surface waters, but the extent of enhancement is less than that in DI water. This is because that the increase of $k_{obs-RBV}$ mainly come from the oxidation of RBV by $TEMPO^+$ and PINO. As discussed above, the generations of $TEMPO^+$ and PINO deeply depend on the existence of radicals. The DOM in actual waters could inhibit the generation of $TEMPO^+$ and PINO by scavenging the radicals, which would weaken the RBV degradation.

3.6. Products and toxicity

The proposed pathways for RBV degradation by UV/Chlorine and UV/Chlorine/Redox mediators processes are illustrated in Fig. 10. RBV (P1, m/z = 245.09) molecule contains Furan ring structure that tends to be halogenated via electrophilic substitution reaction [65]. Pathway 1 refers to RBV degradation by free chlorine only process, Pathway 2 refers to RBV degradation by UV/Chlorine process, and Pathway 3 and 4 refer to RBV degradation by UV/Chlorine/TEMPO and UV/Chlorine/NHPI processes, respectively.

In Pathway 1, the hydroxyl groups at C4 and C6 are substituted by

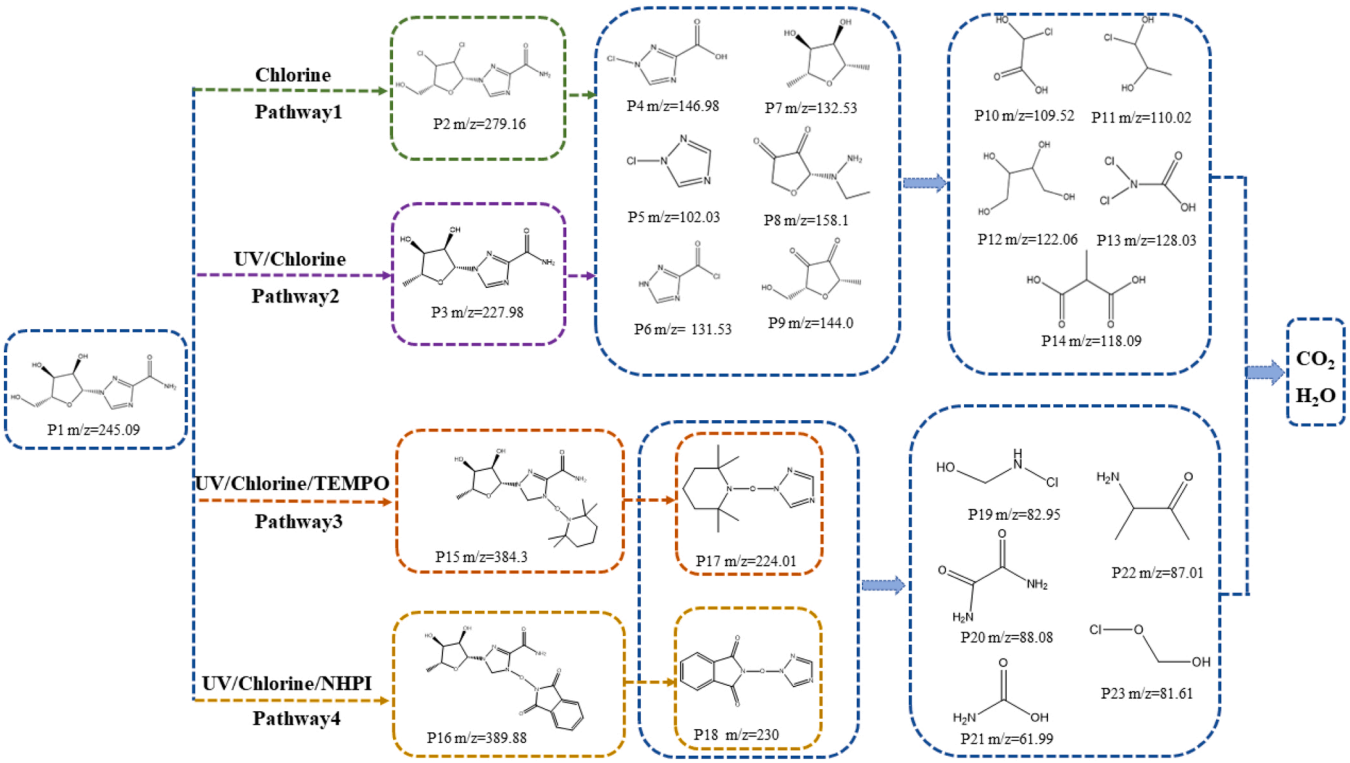

Fig. 10. The proposed degradation pathways of RBV in different degradation processes.

chlorine atoms through oxidation, which generates initial RBV oxidation products P2 ($m/z = 279.16$). In addition, the electron cloud density of Furan ring structure is decreased after its oxidation, and the C8 of RBV molecule connects with a Pyridine ring structure. This leads to the decrease of N-C bond energy between C8 and N10, which will then be broken by free chlorine to generate single ring products (P4-P9). Afterward, free chlorine will further oxidize and open the ring of Furan and Pyridine structures to generate P10-P14.

In Pathway 2, free chlorine is excited by UV photon to generate HO• and RCSs, which will break the bond between O1 and C2 on RBV molecule to form P3 ($m/z = 227.98$). Additionally, single ring products (P4-P9) and ring open products (P10-P14) were identified by LC-MS-MS spectra after a short time of UV treatment, indicating that the oxidation of organic compound by UV/Chlorine process is more complete than that by Chlorine only process. Furthermore, the redox mediator substitute products of RBV (P15, $m/z = 384.3$ and P16, $m/z = 389.88$) were identified after the two redox mediators were added into UV/Chlorine process (Pathway 3 and Pathway 4), which confirmed the inference that the reactive intermediates derived from redox mediators could contribute to RBV photodegradation by reacting with RBV.

The substitution by free chlorine will affect the electron cloud densities of Furan and Pyridine rings. Thus, it can be inferred that $TEMPO^+$ and PINO will react with the heterocyclic structure on RBV molecule, whose electron cloud conjugated structure is changed by chlorine substitution. Then, the number of active sites (easily react with radicals) increases with the proceeding of oxidation and attacks by $TEMPO^+$ and PINO, which promotes the bond break between the two heterocyclic structures and open of rings to yield P17-P23 [66,67]. According to the HOMO orbital model (Fig.S17), there are lots of electron rich groups in RBV molecule that contain plenty of active sites, leading to diversified RBV products. When comparing the RBV products from UV/Chlorine process with and without redox mediators, the molecular weights of the products from UV/Chlorine/redox mediator processes are much lower, indicating that redox mediators promote not only the rate, but also the degree of RBV degradation.

Quantitative Structure Activity Relationship (QSAR) coupling with ECOSAR software was used to assess the toxicity of RBV and its products. The results are summarized in Table S3 and Table S4 [68,69]. In terms of acute toxicity, although the median lethal concentration (LC50) of intermediate transformation products (P2-P8) are lower than that of RBV, the LC50 of most end products to fish and algae are higher than that of RBV, indicating that the acute toxicities to fish and algae are reduced after the final degradation of RBV. In terms of chronic toxicity, the difference between different organisms is smaller than that of acute toxicity. Similar to acute toxicity, the chronic toxicities of the products to fish and algae are lower than those to Daphnia.

After the UV/Chlorine process with and without redox mediators, the acute toxicities of the RBV final products to fish are provided in Fig. 11. The toxicities of all products (except P11) from UV/Chlorine and UV/Chlorine/Redox mediators processes are lower than that of RBV, whereas the toxicity of P11 from UV/Chlorine process is higher than that of RBV. These results demonstrate that the toxicities of the products from UV/Chlorine process are higher than RBV, and the toxicities of the products UV/Chlorine/Redox mediator processes are lower than their parent compound. As a result, introducing redox mediators into UV/Chlorine process will not only promote the degradation of RBV, but also reduce the toxicities of its products.

4. Conclusions

This work focused on revealing the roles that trace amount N-oxyl compounds (TEMPO and NHPI) play in the RBV degradation by UV/Chlorine process as redox mediators. The degradation kinetics in waters with different pH, DOM concentrations, anion concentrations, and actual surface water matrices indicated that redox mediators can always enhance RBV abatement by UV/Chlorine process in the pH range of 4.0–10.0 or in actual surface water matrices, where the rate of RBV degradation in DI water with neutral pH significantly increased by 30% and 52% after adding TEMPO and NHPI into UV/Chlorine process, respectively. However, the enhancement of TEMPO and NHPI on RBV

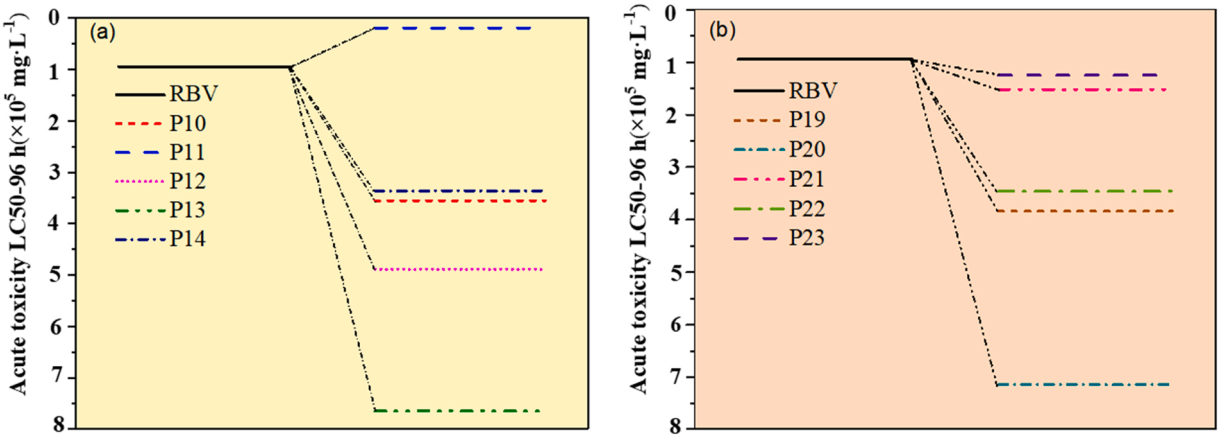

Fig. 11. Acute toxicity assessment for fish of RBV and its products in different treatment processes. (a) UV/Chlorine process; (b) UV/Chlorine/redox mediator process.

degradation by UV/Chlorine process varied with the pH of reactive solution, and DOM, HCO_3^-, as well as Cl^- could weaken the promotion of redox mediators on RBV abatement by reducing the reactive intermediates. The results of probe compounds and scavenging experiments indicate that HO• contributed most to the photodegradation of RBV. TEMPO and NHPI enhanced the RBV degradation by UV/Chlorine process through their oxidation products ($TEMPO^+$ and PINO) that could degrade RBV by oxidizing secondary hydroxyl group into carbonyl group or extracting hydrogen atom. TEMPO and NHPI could inhibit the generation of ClO• in UV/Chlorine process, and the generation of $TEMPO^+$ and PINO deeply relied on the existence of HO• and RCSs. The analyses on the products of RBV degradation and their LC50 for aquatic organisms suggested that the N-oxyl redox mediators could also promote the detoxification of RBV and its products by UV/Chlorine process.

CRediT authorship Contribution statement

Qiyuan Sun: Research plan, Data processing, Investigation, Software, Writing – original draft preparation, Funding acquisition; **Jing Yang:** Most of photodegradation experiment operation and software; **Yongjie Fan:** RBV degradation products detection; **Kaicong Cai:** Data processing and software; Zhilei Lu and Zhenle He: Probable compounds detection; **Zeping Xu and Xingteng Lai:** Radical scavenging experiment; **Yuyi Zheng and Changqing Liu:** Toxicity assessment of RBV products; **Feifeng Wang:** Validation, Writing review & editing; **Zhe Sun:** Validation, Writing – review & editing.

Declaration of Competing Interest

The authors declare that they have no known competing financial interests or personal relationships that could have appeared to influence the work reported in this paper.

Data availability

The authors are unable or have chosen not to specify which data has been used.

Acknowledgements

This work was supported financially by the Natural Science Foundation of China [grant number 52070044]; Natural Science Foundation of Fujian Province [grant number 2021J06022, 2021J01201].

Appendix A. Supporting information

Supplementary data associated with this article can be found in the online version at doi:10.1016/j.apcatb.2022.121709.

References

[1] World Health Organization, Clinical Management of Severe Acute Respiratory InfectionWhen Novel Coronavirus (2019-nCoV) Infection Is Suspected: InterimGuidance. 2020.
[2] X. Chen, L. Lei, S. Liu, J. Han, R. Li, J. Men, L. Li, L. Wei, Y. Sheng, L. Yang, B. Zhou, L. Zhu, Occurrence and risk assessment of pharmaceuticals and personal care products (PPCPs) against COVID-19 in lakes and WWTP-river-estuary system in Wuhan, China, Sci. Total. Environ. 792 (2021), 148352, https://doi.org/10.1016/j.scitotenv.2021.148352.
[3] K. Kuroda, C. Li, K. Dhangar, M. Kumar, Predicted occurrence, ecotoxicological risk and environmentally acquired resistance of antiviral drugs associated with COVID-19 in environmental waters, Sci. Total. Environ. 776 (2021), 145740, https://doi.org/10.1016/j.scitotenv.2021.145740.
[4] M. Kumari, A. Kumar, Environmental and human health risk assessment of mixture of Covid-19 treating pharmaceutical drugs in environmental waters, Sci. Total. Environ. 812 (2022), 152485, https://doi.org/10.1016/j.scitotenv.2021.152485.
[5] X. Liu, Y. Hong, S. Ding, W. Jin, S. Dong, R. Xiao, W. Chu, Transformation of antiviral ribavirin during ozone/PMS intensified disinfection amid COVID-19 pandemic, Sci. Total. Environ. 790 (2021), 148030, https://doi.org/10.1016/j.scitotenv.2021.148030.
[6] X.Y. Hu, J. Fan, K.L. Zhang, N. Yu, J.J. Wang, Pharmaceuticals removal by novel nanoscale photocatalyst Bi4VO8Cl: influencing factors, kinetics, and mechanism, Ind. Eng. Chem. Res. 53 (2014) 14623–14632, https://doi.org/10.1021/ie501855r.
[7] M. Chen, J. Lu, J. Gao, C. Yu, W. Xing, J. Dai, M. Meng, Y. Yan, Y. Wu, Design of self-cleaning molecularly imprinted membrane with antibacterial ability for high-selectively separation of ribavirin, J. Membr. Sci. 642 (2022), 119994, https://doi.org/10.1016/j.memsci.2021.119994.
[8] S. Zhou, Y. Wang, K. Zhou, D. Ba, Y. Ao, P. Wang, In-situ construction of Z-scheme g-C3N4/WO3 composite with enhanced visible-light responsive performance for nitenpyram degradation, Chin. Chem. Lett. 32 (2021) 2179–2182, https://doi.org/10.1016/j.cclet.2020.12.002.
[9] Y. Yeom, J. Han, X. Zhang, C. Shang, T. Zhang, X. Li, X. Duan, D.D. Dionysiou, A review on the degradation efficiency, DBP formation, and toxicity variation in the UV/chlorine treatment of micropollutants, Chem. Eng. J. 424 (2021), 130053, https://doi.org/10.1016/j.cej.2021.130053.
[10] T. Zhang, Y. Chen, Y. Wang, J. Le Roux, Y. Yang, J.-P. Croué, Efficient peroxydisulfate activation process not relying on sulfate radical generation for water pollutant degradation, Environ. Sci. Technol. 48 (2014) 5868–5875, https://doi.org/10.1021/es501218f.
[11] X. Duan, H. Sun, Y. Wang, J. Kang, S. Wang, N-doping-induced nonradical reaction on single-walled carbon nanotubes for catalytic phenol oxidation, ACS Catal. 5 (2015) 553–559, https://doi.org/10.1021/cs5017613.
[12] P. Duan, J. Pan, W. Du, Q. Yue, B. Gao, X. Xu, Activation of peroxymonosulfate via mediated electron transfer mechanism on single-atom Fe catalyst for effective organic pollutants removal, Appl. Catal. B-Environ. 299 (2021), 120714, https://doi.org/10.1016/j.apcatb.2021.120714.
[13] Z. Wan, Y. Sun, D.C.W. Tsang, Z. Xu, E. Khan, S.-H. Liu, X. Cao, Sustainable impact of tartaric acid as electron shuttle on hierarchical iron-incorporated biochar, Chem. Eng. J. 395 (2020), 125138, https://doi.org/10.1016/j.cej.2020.125138.
[14] J. Lin, Y. Hu, J. Xiao, Y. Huang, M. Wang, H. Yang, J. Zou, B. Yuan, J. Ma, Enhanced diclofenac elimination in Fe(II)/peracetic acid process by promoting Fe

(III)/Fe(II) cycle with ABTS as electron shuttle, Chem. Eng. J. 420 (2021), 129692, https://doi.org/10.1016/j.cej.2021.129692.
[15] K. Xu, H. Dong, M. Li, Z. Qiang, Quinone group enhances the degradation of levofloxacin by aqueous permanganate: kinetics and mechanism, Water Res 143 (2018) 109–116, https://doi.org/10.1016/j.watres.2018.06.026.
[16] Y. Song, J. Jiang, J. Ma, S.-Y. Pang, Y.-z Liu, Y. Yang, C.-w Luo, J.-q Zhang, J. Gu, W. Qin, ABTS as an electron shuttle to enhance the oxidation kinetics of substituted phenols by aqueous permanganate, Environ. Sci. Technol. 49 (2015) 11764–11771, https://doi.org/10.1021/acs.est.5b03358.
[17] Z. Shi, C. Jin, R. Bai, Z. Gao, J. Zhang, L. Zhu, Z. Zhao, T.J. Strathmann, Enhanced transformation of emerging contaminants by permanganate in the presence of redox mediators, Environ. Sci. Technol. 54 (2020) 1909–1919, https://doi.org/10.1021/acs.est.9b05711.
[18] T. Janoschka, N. Martin, M. Hager, U.S. Schubert, An Aqueous Redox-Flow Battery with High Capacity and Power: The TEMPTMA/MV System, Angew. Chem. Int. Edit. 55 (2016) 14427–14430, https://doi.org/10.1002/anie.201606472.
[19] J.E. Nutting, M. Rafiee, S.S. Stahl, Tetramethylpiperidine N-Oxyl (TEMPO), Phthalimide N-Oxyl (PINO), and related N-Oxyl species: electrochemical properties and their use in electrocatalytic reactions, Chem. Rev. 118 (2018) 4834–4885, https://doi.org/10.1021/acs.chemrev.7b00763.
[20] I. Bosque, G. Magallanes, M. Rigoulet, M.D. Kärkäs, C.R.J. Stephenson, Redox catalysis facilitates lignin depolymerization, ACS Cent. Sci. 3 (2017) 621–628, https://doi.org/10.1021/acscentsci.7b00140.
[21] M. Rafiee, F. Wang, D.P. Hruszkewycz, S.S. Stahl, N-Hydroxyphthalimide-mediated electrochemical iodination of methylarenes and comparison to electron-transfer-initiated C–H functionalization, J. Am. Chem. Soc. 140 (2018) 22–25, https://doi.org/10.1021/jacs.7b09744.
[22] F. Recupero, C. Punta, Free radical functionalization of organic compounds catalyzed by N-hydroxyphthalimide, Chem. Rev. 107 (2007) 3800–3842, https://doi.org/10.1021/cr040170k.
[23] N.I. Kuznetsova, D.E. Babushkin, V.N. Zudin, O.S. Koscheeva, L.I. Kuznetsova, Low-temperature oxidation of isopropylbenzene mediated by the system of NHPI, Fe (acac)3 and 1,10-phenanthroline, Catal. Commun. 149 (2021), 106218, https://doi.org/10.1016/j.catcom.2020.106218.
[24] X.Q. Guo, R.A. Mittelstaedt, L. Guo, J.G. Shaddock, R.H. Heflich, A.H. Bigger, M. M. Moore, N. Mei, Nitroxide TEMPO: a genotoxic and oxidative stress inducer in cultured cells, Toxicol. . Vitr. 27 (2013) 1496–1502, https://doi.org/10.1016/j.tiv.2013.02.019.
[25] X.Q. Guo, S. Chen, Z.H. Zhang, V.N. Dobrovolsky, S.L. Dial, L. Guo, N. Mei, Reactive oxygen species and c-Jun N-terminal kinases contribute to TEMPO-induced apoptosis in L5178Y cells, Chem. -Biol. Interact. 235 (2015) 27–36, https://doi.org/10.1016/j.cbi.2015.04.009.
[26] M. Wang, A. Zhou, T. An, L. Kong, C. Yu, J. Liu, C. Xia, H. Zhou, Y. Li, N-Hydroxyphthalimide exhibits antitumor activity by suppressing mTOR signaling pathway in BT-20 and LoVo cells, J. Exp. Clin. Canc. Res. 35 (2016) 41, https://doi.org/10.1186/s13046-016-0315-1.
[27] F. Li, C.-H. Huang, L.-N. Xie, N. Qu, J. Shao, B. Shao, B.-Z. Zhu, An exceptionally facile two-step structural isomerization and detoxication via a water-assisted double lossen rearrangement, Sci. Rep. UK 6 (2016) 39207, https://doi.org/10.1038/srep39207.
[28] J.R. Bolton, K.G. Linden, Standardization of methods for fluence "UV dose… determination in bench-scale UV experiments, J. Environ. Eng. 129 (2003) 209–216, https://doi.org/10.1061/ASCE0733-93722003129:3209.
[29] R. Yin, E.R. Blatchley, 3rd, C. Shang, UV photolysis of mono- and dichloramine using UV-LEDs as radiation sources: photodecay rates and radical concentrations, Environ. Sci. Technol. 54 (2020) 8420–8429, https://doi.org/10.1021/acs.est.0c01639.
[30] G. Chen, W. Shi, M. Xia, W. Lei, F. Wang, X. Gong, Theoretical study of solvent effects on RDX crystal quality and sensitivity using an implicit solvation model, J. Mol. Model. 20 (2014) 2326, https://doi.org/10.1007/s00894-014-2326-1.
[31] X.-H. Yi, H. Ji, C.-C. Wang, Y. Li, Y.-H. Li, C. Zhao, A. Wang, H. Fu, P. Wang, X. Zhao, W. Liu, Photocatalysis-activated SR-AOP over PDINH/MIL-88A(Fe) composites for boosted chloroquine phosphate degradation: Performance, mechanism, pathway and DFT calculations, Appl. Catal. B-Environ. 293 (2021), 120229, https://doi.org/10.1016/j.apcatb.2021.120229.
[32] X.R. Zhang, J. Li, J.Y. Yang, K.V. Wood, A.P. Rothwell, W. Li, E.R. Blatchley Iii, Chlorine/UV process for decomposition and detoxification of microcystin-LR, Environ. Sci. Technol. 50 (2016) 7671–7678, https://doi.org/10.1021/acs.est.6b02009.
[33] J. Fang, Y. Fu, C. Shang, The roles of reactive species in micropollutant degradation in the UV/free chlorine system, Environ. Sci. Technol. 48 (2014) 1859–1868, https://doi.org/10.1021/es4036094.
[34] J.E. Grebel, J.J. Pignatello, W.A. Mitch, Impact of halide ions on natural organic matter-sensitized photolysis of 17beta-estradiol in saline waters, Environ. Sci. Technol. 46 (2012) 7128–7134, https://doi.org/10.1021/es3013613.
[35] Y. Lei, X. Lei, P. Westerhoff, X. Zhang, X. Yang, Reactivity of chlorine radicals (Cl• and Cl2•–) with dissolved organic matter and the formation of chlorinated byproducts, Environ. Sci. Technol. 55 (2021) 689–699, https://doi.org/10.1021/acs.est.0c05596.
[36] P. Sun, T. Meng, Z. Wang, R. Zhang, H. Yao, Y. Yang, L. Zhao, Degradation of organic micropollutants in UV/NH2Cl advanced oxidation process, Environ. Sci. Technol. 53 (2019) 9024–9033, https://doi.org/10.1021/acs.est.9b00749.
[37] S. Wang, J. Wu, X. Lu, W. Xu, Q. Gong, J. Ding, B. Dan, P. Xie, Removal of acetaminophen in the Fe2+/persulfate system: Kinetic model and degradation pathways, Chem. Eng. J. 358 (2019) 1091–1100, https://doi.org/10.1016/j.cej.2018.09.145.
[38] H. Zhang, Z. Shi, R. Bai, D. Wang, F. Cui, J. Zhang, T.J. Strathmann, Role of TEMPO in enhancing permanganate oxidation toward organic contaminants, Environ. Sci. Technol. 55 (2021) 7681–7689, https://doi.org/10.1021/acs.est.1c01824.
[39] J. Li, Z. Li, Y. Yang, B. Kong, C. Wang, Laboratory study on the inhibitory effect of free radical scavenger on coal spontaneous combustion, Fuel Process. Technol. 171 (2018) 350–360, https://doi.org/10.1016/j.fuproc.2017.09.027.
[40] G. Nardi, I. Manet, S. Monti, M.A. Miranda, V. Lhiaubet-Vallet, Scope and limitations of the TEMPO/EPR method for singlet oxygen detection: the misleading role of electron transfer, Free. Radic. Biol. Med. 77 (2014) 64–70, https://doi.org/10.1016/j.freeradbiomed.2014.08.020.
[41] X. Baucherel, L. Gonsalvi, I.W.C.E. Arends, S. Ellwood, R.A. Sheldon, Aerobic oxidation of cycloalkanes, alcohols and ethylbenzene catalyzed by the novel carbon radical chain promoter NHS (N-Hydroxysaccharin), Adv. Synth. Catal. 346 (2004) 286–296, https://doi.org/10.1002/adsc.200303197.
[42] Z. Liu, H. Lan, Y. Wang, J. Zhang, J. Qin, R. Zhang, N. Dong, Highly efficient degradation of bisphenol A with persulfate activated by vacuum-ultraviolet/ultraviolet light (VUV/UV): experiments and theoretical calculations, Chem. Eng. J. 429 (2022), 132485, https://doi.org/10.1016/j.cej.2021.132485.
[43] C. Yang, L.A. Farmer, D.A. Pratt, S. Maldonado, C.R.J. Stephenson, Mechanism of electrochemical generation and decomposition of phthalimide-N-oxyl, J. Am. Chem. Soc. 143 (2021) 10324–10332, https://doi.org/10.1021/jacs.1c04181.
[44] Y.G. Feng, D.W. Smith, J.R. Bolton, Photolysis of aqueous free chlorine species (NOCl and OCl-) with 254 nm ultraviolet light, J. Environ. Eng. Sci. 6 (2007) 277–284, https://doi.org/10.1139/s06-052.
[45] Y. Pan, S. Cheng, X. Yang, J. Ren, J. Fang, C. Shang, W. Song, L. Lian, X. Zhang, UV/chlorine treatment of carbamazepine: Transformation products and their formation kinetics, Water Res. 116 (2017) 254–265, https://doi.org/10.1016/j.watres.2017.03.033.
[46] X.R. Zhang, J. He, S.Q. Xiao, X. Yang, Elimination kinetics and detoxification mechanisms of microcystin-LR during UV/Chlorine process, Chemosphere 214 (2019) 702–709, https://doi.org/10.1016/j.chemosphere.2018.09.162.
[47] Y.H. Chuang, S. Chen, C.J. Chinn, W.A. Mitch, Comparing the UV/Monochloramine and UV/Free chlorine advanced oxidation processes (AOPs) to the UV/Hydrogen Peroxide AOP under scenarios relevant to potable reuse, Environ. Sci. Technol. 51 (2017) 13859–13868, https://doi.org/10.1021/acs.est.7b03570.
[48] J. Jiang, S.Y. Pang, J. Ma, Oxidation of triclosan by permanganate (Mn(VII)): importance of ligands and in situ formed manganese oxides, Environ. Sci. Technol. 43 (2009) 8326–8331, https://doi.org/10.1021/es901663d.
[49] B. Sun, J. Zhang, J.S. Du, J.L. Qiao, X.H. Guan, Reinvestigation of the role of humic acid in the oxidation of phenols by permanganate, Environ. Sci. Technol. 47 (2013) 14332–14340, https://doi.org/10.1021/es404138s.
[50] J.S. Du, B. Sun, J. Zhang, X.H. Guan, Parabola-like shaped pH-rate profile for phenols oxidation by aqueous permanganate, Environ. Sci. Technol. 46 (2012) 8860–8867, https://doi.org/10.1021/es302076s.
[51] P.Z. Sun, W.N. Lee, R.C. Zhang, C.H. Huang, Degradation of DEET and caffeine under UV/chlorine and simulated sunlight/chlorine conditions, Environ. Sci. Technol. 50 (2016) 13265–13273, https://doi.org/10.1021/acs.est.6b02287.
[52] K. Guo, Z. Wu, C. Shang, B. Yao, S. Hou, X. Yang, W. Song, J. Fang, Radical chemistry and structural relationships of PPCP degradation by UV/Cchlorine treatment in simulated drinking water, Environ. Sci. Technol. 51 (2017) 10431–10439, https://doi.org/10.1021/acs.est.7b02059.
[53] L. Jia, K. Chen, C. Wang, J. Yao, Z. Chen, H. Li, Unexpected oxidation of β-isophorone with molecular oxygen promoted by TEMPO, RSC Adv. 4 (2014) 15590, https://doi.org/10.1039/c3ra47901c.
[54] L. Wang, B. Li, D.D. Dionysiou, B. Chen, J. Yang, J. Li, Overlooked formation of H2O2 during the hydroxyl radical-scavenging process when using alcohols as scavengers, Environ. Sci. Technol. 56 (2022) 3386–3396, https://doi.org/10.1021/acs.est.1c03796.
[55] Y. Ma, C. Loyns, P. Price, V. Chechik, Thermal decay of TEMPO in acidic media via an N-oxoammonium salt intermediate, Org. Biomol. Chem. 9 (2011) 5573–5578, https://doi.org/10.1039/c1ob05475a.
[56] C.F. Zhang, Z.P. Huang, J.M. Lu, N.C. Luo, F. Wang, Generation and confinement of long-lived N-oxyl radical and its photocatalysis, J. Am. Chem. Soc. 140 (2018) 2032–2035, https://doi.org/10.1021/jacs.7b12928.
[57] C. Annunziatini, M.F. Gerini, O. Lanzalunga, M. Lucarini, Aerobic oxidation of benzyl alcohols catalyzed by aryl substituted N-hydroxyphthalimides. Possible involvement of a charge-transfer complex, J. Org. Chem. 69 (2004) 3431–3438, https://doi.org/10.1021/jo049887y.
[58] H.Y. Liu, Z.C. Hou, Y.J. Li, Y.J. Lei, Z.H. Xu, J.J. Gu, S.L. Tian, Modeling degradation kinetics of gemfibrozil and naproxen in the UV/chlorine system: Roles of reactive species and effects of water matrix, Water Res 202 (2021), 117445, https://doi.org/10.1016/j.watres.2021.117445.
[59] M.K. Kim, K.D. Zoh, Effects of natural water constituents on the photo-decomposition of methylmercury and the role of hydroxyl radical, Sci. Total. Environ. 449 (2013) 95–101, https://doi.org/10.1016/j.scitotenv.2013.01.039.
[60] Y.Y. Xiang, J.Y. Fang, C. Shang, Kinetics and pathways of ibuprofen degradation by the UV/chlorine advanced oxidation process, Water Res 90 (2016) 301–308, https://doi.org/10.1016/j.watres.2015.11.069.
[61] C.Y. Hu, C. Xiong, Y.L. Lin, Y.Y. Zhu, Q.B. Wang, L. Xu, D.D. Huang, Degradation of 2-phenylbenzimidazole 5-sulfonic acid by UV/chlorine advanced oxidation technology: Kinetic model, degradation byproducts and reaction pathways, J. Hazard. Mater. 431 (2022), 128574, https://doi.org/10.1016/j.jhazmat.2022.128574.
[62] B. Sun, Y.Z. Zheng, C. Shang, R. Yin, Concentration-dependent chloride effect on radical distribution and micropollutant degradation in the sulfate radical-based

AOPs, J. Hazard. Mater. 430 (2022), 128450, https://doi.org/10.1016/j.jhazmat.2022.128450.
[63] H. Liu, B. Zhang, Y. Li, Q. Fang, Z. Hou, S. Tian, J. Gu, Effect of radical species and operating parameters on the degradation of sulfapyridine using a UV/chlorine system, Ind. Eng. Chem. Res. 59 (2020) 1505–1516, https://doi.org/10.1021/acs.iecr.9b06228.
[64] J. Wenk, U. von Gunten, S. Canonica, Effect of dissolved organic matter on the transformation of contaminants induced by excited triplet states and the hydroxyl radical, Environ. Sci. Technol. 45 (2011) 1334–1340, https://doi.org/10.1021/es102212t.
[65] L.M. Pevzner, Synthesis of 3,4-disubstituted phosphorus-containing furans with free 2 and 5 positions, Russ. J. Gen. Chem. 71 (2001) 565–567, https://doi.org/10.1023/a:1012366731221.
[66] Y. Pan, X. Li, K. Fu, Z. Gu, J. Shi, H. Deng, Overlooked role of secondary radicals in the degradation of beta-blockers and toxicity change in UV/chlorine process, Chem. Eng. J. 391 (2020), 123606, https://doi.org/10.1016/j.cej.2019.123606.
[67] Y. Wang, H. Dong, W. Qin, J. Li, Z. Qiang, Activation of organic chloramine by UV photolysis: a non-negligible oxidant for micro-pollutant abatement and disinfection by-product formation, Water Res 207 (2021), 117795, https://doi.org/10.1016/j.watres.2021.117795.
[68] J. Kuang, J. Huang, B. Wang, Q. Cao, S. Deng, G. Yu, Ozonation of trimethoprim in aqueous solution: identification of reaction products and their toxicity, Water Res 47 (2013) 2863–2872, https://doi.org/10.1016/j.watres.2013.02.048.
[69] H.F. Miao, M. Cao, D.Y. Xu, H.Y. Ren, M.X. Zhao, Z.X. Huang, W.Q. Ruan, Degradation of phenazone in aqueous solution with ozone: influencing factors and degradation pathways, Chemosphere 119 (2015) 326–333, https://doi.org/10.1016/j.chemosphere.2014.06.082.